Single cell microwave biosensor for monitoring cellular response to electrochemotherapy

Amar Tamra, Amel Zedek, Marie-Pierre Rols, David Dubuc, Katia Grenier

Single Cell Microwave Biosensor for Monitoring Cellular Response to Electrochemotherapy

A. Tamra, A. Zedek, M-P. Rols, D. Dubuc, and K. Grenier

***Abstract*—This paper presents a 40 GHz microwave biosensor used to monitor and characterize single cells (THP-1) subjected to electrochemotherapy and obtain an electronic signature of the treatment efficiency. This biosensor proposes a non-destructive and label-free technique that first allows, with the rapid measurement of single untreated cells in their culture medium, the extraction of two frequency-dependent dielectric parameters, the capacitance (C (f)) and the conductance (G (f)). Second, this technique can powerfully reveal the effects of a chemical membrane permeabilizing treatment (Saponin). At last, it permits us to detect, and predict, the potentiation of a molecule classically used in chemotherapy (Bleomycin) when combined with the application of electric pulses (principle of electrochemotherapy). Treatment-affected cells show a decrease in the capacitive and conductive contrasts, indicating damages at the cellular levels. Along with these results, classical biological tests are conducted. Statistical analysis points out a high correlation rate (R^2>0.97), which clearly reveals the reliability and efficacy of our technique and makes it an attractive technique for biology related researches and personalized medicine.**

***Index Terms*—Biosensor, Electrochemotherapy, Microwave dielectric spectroscopy, Single Cell, THP-1 cells**

I. Introduction

ELECTROCHEMOTHERAPY (ECT) is a local antitumor treatment that combines the administration of chemotherapeutic drugs with the local application of electric field pulses in order to transiently depolarize the cell membrane, making it permeable, and thus facilitate the delivery of non-permeant or low permeant drugs into cancer cells [1]–[3]. Among chemotherapeutic agents, bleomycin and cisplatin are the best potential candidates for ECT in cancer patients [4]. Once passed the cellular membrane and inside the cells, bleomycin induces single and double strand DNA breaks that lead to cell death [5]. The increase in the concentration of the drug in the tumor cells (300-700 fold) [6] allows the dramatic increase of the cytotoxicity of the molecule locally, at the site of the electroporation and leads to neoplastic cell death. The healthy cells of the tissues surrounding the tumor nodules, which are not subjected to electroporation pulses, are protected from toxic action. This local control of the tumor prolongs the lifespan and improves the quality of life of the patients [7]. In addition to drug-induced cell destruction, electroporation is responsible for vascular changes in the tumor region. A "vascular lock" effect is induced where blood stops flowing though the tissue that has been electroporated [8]. This vascular blocking effect seems to last longer in tumor tissues than in normal ones [9]. After first successful *in vitro* studies [10], ECT has been successfully applied in the first clinical trial, performed in 1990 [11]. Electrochemotherapy is mainly used in treatment of cutaneous and subcutaneous cancers [12]. ECT induces a local yet robust immune response that is responsible for its high effectiveness [13]. It is also of great interest for people diagnosed with cutaneous malignancies at advanced ages as it offers an efficient, safe nonsurgical treatment [14]. Research is still ongoing for treatment of deep-seated tumors such as colorectal cancer [15] and liver metastases [16]. Other modalities, such as calcium electroporation, where cytotoxic drugs are replaced by high concentration level of calcium, also showed great promise [17]. In clinical assays, it is crucial to use the optimal electrical parameters along with the convenient drug concentrations, in order to obtain the desired effect while minimizing the side effects and the damage of the healthy cells. This comes from the significant differences between different tumor cell types and different patients phenotypes. From here comes the urge to deepen the research on the effects of ECT with various drugs on different cell types.

Many researches are now focalizing on transposing electroporation studies “on-chip” [18]–[22] in order to avoid costly, time-consuming work and invasiveness of the routinely used methods, such as microscopy, flow cytometry and chemical tests. Although very effective, there is an ongoing trend to develop and employ new analysis methods [20], [23]–

This work was supported in part by the the Toulouse COMUE and the Region Midi-Pyrénées in France and in part by LAAS-CNRS micro and nano technologies platform, a member of the RENATECH French national network.

D. Dubuc and *K. Grenier are with the National Scientific Research Center, Laboratory of Analysis and Architecture of Systems, 31031 Toulouse, France (phone: +33 56133 6291; fax: +33 56133 6969; correspondence e-mail: grenier@laas.fr).

*M-P. Rols are with the Institute of Pharmacology and Structural Biology, 31077, Toulouse, France (phone: +33 56117 5811; fax: +33 56117 5994; correspondence e-mail: rols@ipbs.fr).

A. Tamra was with the National Scientific Research Center, Laboratory of Analysis and Architecture of Systems and the Institute of Pharmacology and Structural Biology, Toulouse, France. She is now with the King Abdullah University of Science and Technology, Saudi Arabia.

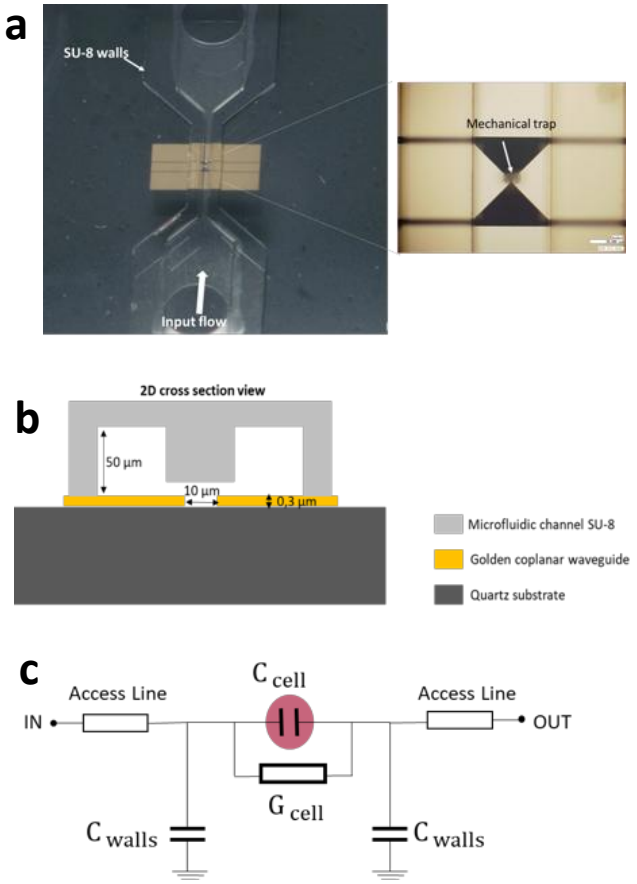

Fig. 1. Microwave biosensor. (a) The optical microscope image of the microwave biosensor with a microfluidic channel. (b) 2D cross section view of the biosensor. (c) Associated electric scheme of the device.

[28], among which the electrical spectroscopy analysis. Microwave dielectric spectroscopy (MDS) is a label-free analysis approach that involves applying microwave waves (40 MHz - 40 GHz) to biological samples and measuring their dielectric properties. It has several advantages such as the use of non-ionizing waves for a non-intrusive, direct and contactless analysis. The technique mainly detects changes of the water molecules network and is related to any modification in the ratio of bound water molecules to free ones [29]–[32]. Due to the penetration of electromagnetic waves in the cells in the microwave range, intracellular characterization is accessible either with cell suspensions [29], [30], [33] or at the single cell level [34]–[38]. The MDS technique permits therefore to sense and monitor pathological transformations [31], [32]. In the context of electroporation, it has been used to study the conductivity of the cell suspension [39], the cytoplasm and the nucleoplasm [40] of Jurkat cells exposed to nanosecond electric pulses nsPEF. The kinetic of cells reactions submitted to different electric stresses has also been monitored [41], [42] with microwave signals. However, to our knowledge, there is no work reporting the study of electrochemotherapy effect on biological cells, using MDS analysis.

This work results from our previous paper showing a microwave and microfluidic-based biosensor, able to perform dielectric spectroscopy of the single cell and to monitor the

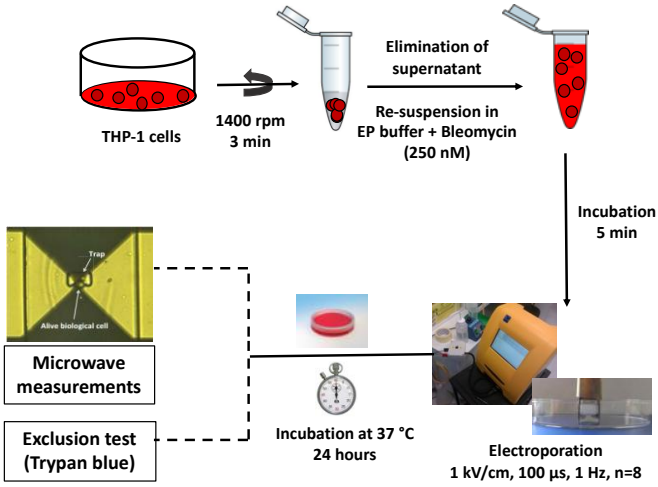

Fig. 2. Biological preparations for the experimental protocol.

intracellular effects of both reversible and irreversible electroporation [41]. In this paper, we present the ability of our biosensor to detect the effects induced by bleomycin treatment coupled with electroporation, i.e. electrochemotherapy, on THP-1 cells. The ultimate goal is to propose a method that can be used in hospital laboratories, which can be applied to evaluate and predict the effect of different types of treatment on cells, in a non-invasive way, without the addition of dyes or fluorochromes.

II. Materials and Methods

A. Description of the microwave biosensor and its fabrication

The MDS biosensor, initially developed by Chen et al. [35], is composed of two different parts (Fig. 1a). The first part is a coplanar waveguide (CPW) that consists in a central golden ribbon (signal) and two ground planes, with a capacitive gap of 10 µm in the center of the central conductor. It is fabricated using an evaporated titanium and gold layer, which is obtained with a lift-off technique and presents a thickness of 0.3 µm. The waveguide is realized on a borosilicate glass substrate, which exhibits low dielectric losses in the microwave range with a loss tangent of 0.0047 and a permittivity of 4.3. On top of the CPW, a 50-µm thick microfluidic channel is perpendicularly placed to the golden waveguide and includes a mechanical trap located just apart the capacitive gap (Fig. 1b). With this trap, one single cell is captured at a time allowing it to interact with the electromagnetic fields, which are focalized in the capacitive gap. Both the microfluidic channel and the trap are fabricated with SU-8 polymer using photolithography technique, whereas the initial technology developed by Chen et al. [35] integrated a fluidic part realized in polydimethylsiloxane (PDMS). The change of fluidic material presents several improvements. The PDMS-elastomer imposes a manual placement of the fluidic part on the microwave sensing electrodes, whereas SU-8 polymer is precisely patterned with photolithographic equipment. The misalignment between the capacitive gap and the cell trap is therefore drastically minimized. In addition, PDMS exhibits

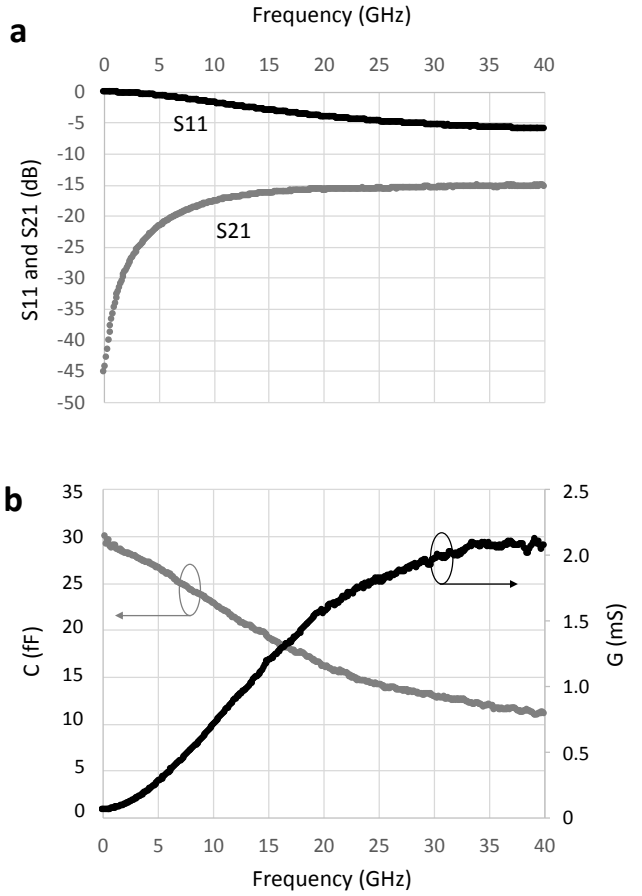

Fig. 3. (a) Measured S parameters and (b) calculated capacitance C and conductance G, while the sensor is loaded by the culture medium.

low stiffness relative to the polymer. While inadvertent sticking of the PDMS blocker to the substrate may occur, the use of a rigid SU-8 structure allows for better microfluidic stability. Primarily, a sacrificial layer of 5 µm thick in LOR photoresist is used to realize the air gap localized at the bottom of the mechanical trap. Its high curing temperature of 180°C enables to stack the subsequent two SU-8 layers, which are deposited and patterned. The first one defines both the cell blocker and the fluidic walls, whereas the second SU-8 layer corresponds to the lid of the fluidic structure. The first SU-8 layer is deposited by spin-coating with conditions suitable to reach a final thickness of 50 µm after hard baking. Once its development is done, the second SU-8 is deposited by rolling. After photolithography and development of the lid, the sacrificial layer is removed by wet etching before drying the structure with ethanol.

The electrical circuit associated with our biosensor is presented in Fig. 1c, where the coplanar waveguide access lines, the SU8 microfluidic walls and the capacitive sensing zone are considered. A de-embedding procedure permits to remove the impact of the access lines and the fluidic walls. Its description is indicated in section 3.1. The individual cell under test is modeled by an electrical circuit, which includes a capacitor C in parallel to a conductance G.

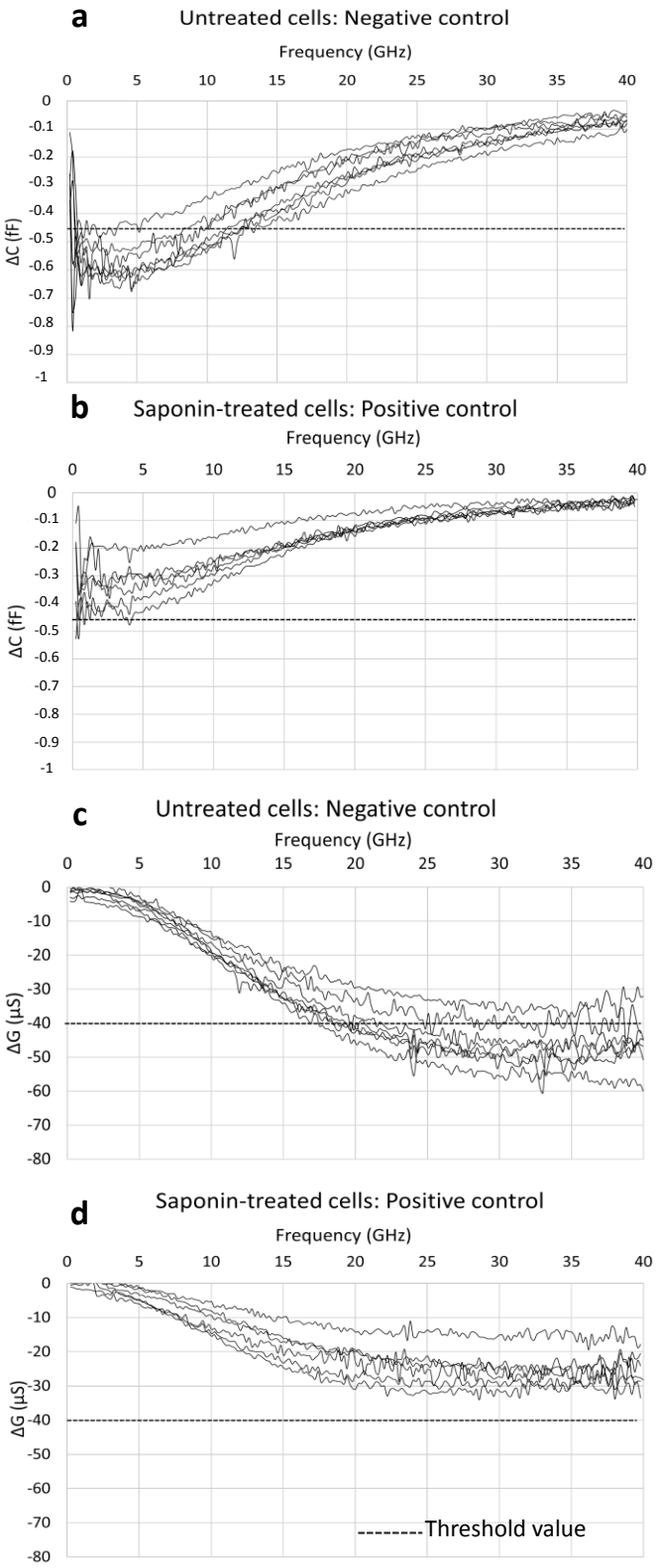

Fig. 4. Capacitive contrast of untreated cells (a) and saponin-treated cells (c). Conductive contrast of untreated cells (b) and saponin-treated cells (d). Cells measurements are performed in culture medium, which serves as reference.

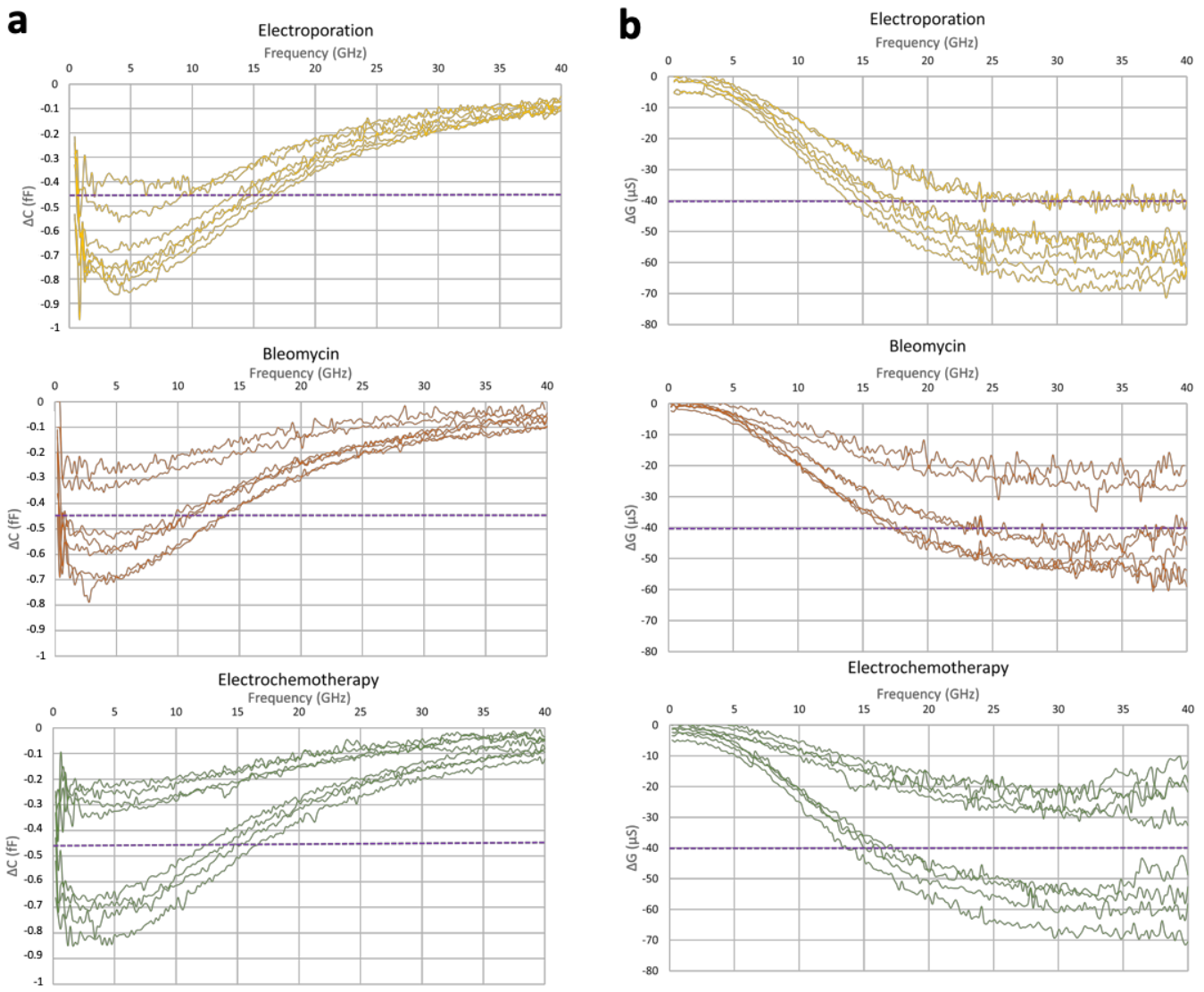

Fig. 5. (a) Capacitive contrast of electroporated cells (yellow color), bleomycin-treated cells (brown) and electrochemotherapy treated cells (green). (b) Conductive contrast of electroporated cells (yellow), bleomycin-treated cells (brown) and electrochemotherapy treated cells (green). Purple dashed lines represent the thresholds.

B. Cells and reagents

In this study, THP-1 cells (ATCC # TIB-202) are employed for three reasons. First, they are human cells derived from monocytic leukemia and constitute an important biological model for studies in oncology. Their electroporation parameters are also known [41]. Finally, as circulating cells, they exhibit a low tendency to aggregate, which is appropriate for analyzing only individual cells in the microwave sensor. They are grown in Roswell Park Memorial Institute Medium (RPMI) (Gibco-Invitrogen, Carlsbad, CA, USA), supplemented with 10% fetal calf serum FCS and a mixture of antibiotics 100 U / ml penicillin and 100 µg / ml streptomycin. The cells are incubated at 37°C under 5% CO_2 for proliferation.

The chemical treatments used are saponin, supplied by Sigma-Aldrich (Lyon, France) and bleomycin, supplied by Merck Millipore (Darmstadt, Germany).

C. Electrochemotherapy

The protocol used is shown in Fig. 2. THP-1 cells are harvested, re-suspended and incubated for 5 minutes in the drug-electroporation buffer mixture. The composition of the buffer is the following, 10 mM K_2HPO_4/KH_2PO_4, 1 mM $MgCl_2$, 250 mM of sucrose, pH 7.4, conductivity 1.7 S/m. The final concentration of the Bleomycin in the solution is 250 nM (250 nMol/L). Eight electric pulses, applied at 1 kV/cm, are generated by a Betatech generator (ELECTRO cell S20, France), where the duration and frequency are fixed as 100 µs and 1 Hz [43]. After electroporation, the cells are incubated with the culture medium for 24 hours, at 37°C. At the end of this incubation time, the cells are either analyzed with the biological exclusion test (Trypan blue test, which is a specific dye that instantly penetrates into the cells with

permeabilized/damaged cytoplasmic membranes), or injected in the microwave biosensor in order to extract the electrical responses. The experiments are carried out in triplicate. Five groups of cells are tested:

1. Untreated cells, negative control
2. Cells with 0.02% saponin, positive control
3. Cells with bleomycin alone (250 nM)
4. Cells with electric pulses alone (1 kV/cm)
5. Cells with ECT (250 nM bleomycin + 1 kV/cm).

D. Microwave measurements

Before proceeding to the microwave measurements, a crucial step of de-embedding is performed, in order to remove the effects of the access lines and the walls and to be able to extract the capacitive and conductive contributions of the cell alone. After injecting and measuring the culture medium alone, which represents the reference medium, the cell suspension is injected in the microfluidic channel. With the help of the mechanical trap, one single cell is blocked right above the sensing zone, whereas all other cells are removed by flushing the culture medium in the fluidic channel. Measurement of S parameters is performed once stabilization is electrically observed. When the sensor is loaded with the culture medium and then with an individual cell, $C_{reference\ medium}$, $G_{reference\ medium}$, and C_{cell} and G_{cell} are extracted respectively. Since C_{cell} and G_{cell} are proportional to the contrasts of the real and imaginary parts of the relative permittivity of the sample, it will therefore be relevant to extract and study these two parameters and their contrast with respect to a reference medium (medium not containing the studied sample: culture medium without cell in our case). This will allow us to observe the changes directly related to the presence of the sample. The differential method is particularly interesting because it takes the drift of the measurement chain over time into account, while improving the repeatability and reproducibility of the tests. As a result, we calculate the capacitive and conductive contrast of the cell relative to the reference medium (culture medium), according to the following equations:

$$\Delta C_{eff} = C_{cell} - C_{reference\ medium} \quad (1)$$

$$\Delta G_{eff} = G_{cell} - G_{reference\ medium}\ . \quad (2)$$

The microwave measurements are performed on wafer in a range of frequencies from 40 MHz to 40 GHz. Further details on the method of extraction of these two readouts could be found in [41]. The contrast spectra obtained at the end of this calculation are presented as a function of frequency. All of the procedures described allow us to perform microwave dielectric spectroscopy MDS, delivering the ΔC and ΔG spectra over a wide frequency range of the microwave domain.

III. Results and Discussion

A. Dielectric properties of THP-1 cells

After having recovered all the measurements of the S parameters, a data processing is applied with Matlab software. It allows us to extract the contrasts of capacitance and conductance as a function of frequency. As an illustration of such data, Fig. 3 (a, b) presents the measured S parameters as well as the extracted capacitance and conductance, while the sensor is loaded by the host medium of the cells. Fig. 4 (a, c) shows, respectively, capacitive contrast (ΔC) and conductive contrast (ΔG) spectra obtained for untreated THP-1 cells. Only a representative number of spectra is shown in all the graphs of this paper. Each spectrum represents the electrical response of a single captured cell over the frequency range from 40 MHz to 40 GHz. As far as the differential method presented earlier is concerned, the corresponding culture medium (RPMI) is considered as the reference. The obtained spectra show that, compared to the culture medium alone, the cell has a significantly different spectral response. Indeed, in living cells, the plasma membrane provides regulation between the intra- and extracellular medium while maintaining a heterogeneity between the concentrations of their constituents. This will result in an increase, in absolute value, of the capacitive and conductive contrasts, resulting from the well-expressed difference between the relatively simple composition of the culture medium, compared to the living

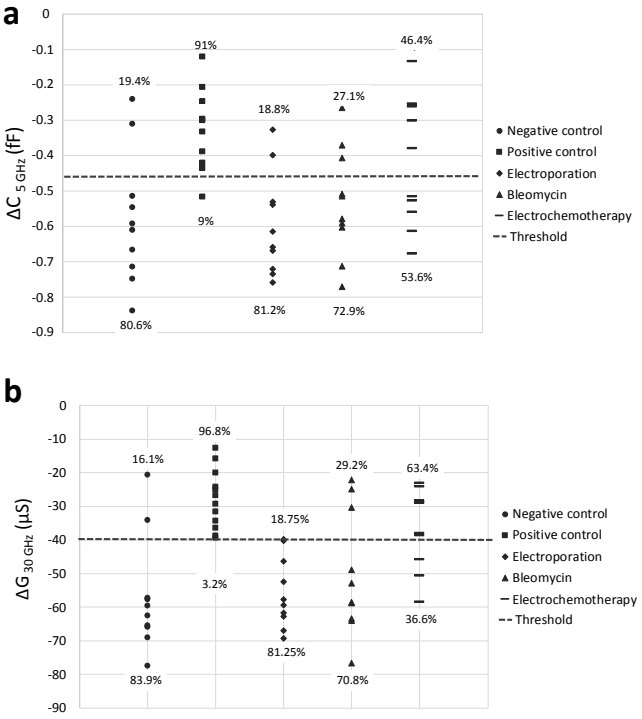

Fig. 6. THP1 response to different treatments estimated by microwave measurements (contrasts of capacitance at 5 GHz and conductance at 30 GHz) and by biological method (exclusion test with trypan blue).

TABLE I
CAPACITIVE CONTRAST $\Delta C_{5\ GHz}$ AND CONDUCTIVE CONTRAST $\Delta C_{30\ GHz}$ OF THP-1 CELLS, ALONG WITH THE THRESHOLD VALUES OF BOTH PARAMETERS

	Untreated THP1	Saponin-treated THP1	Threshold
$\Delta C_{5\ GHz}$ *(fF)*	-0.6 ± 0.1	-0.3 ± 0.077	-0.45
$\Delta G_{30\ GHz}$ *(μS)*	-52 ± 8	-22 ± 7.3	-40

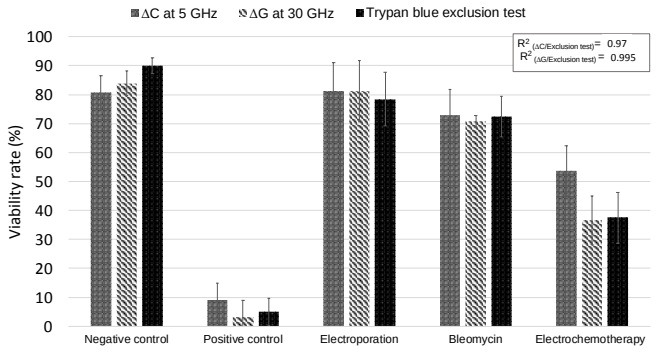

Fig. 7. THP1 response to different treatments estimated by microwave measurements (contrasts of capacitance and conductance) and by biological method (exclusion test with trypan blue).

cell with all its complexity. On the other hand, Fig. 4 (b, d) shows ΔC and ΔG spectra obtained for saponin-treated THP-1 cells (0.02%). Saponins are qualified as detergent molecules because of their ability to solubilize the plasma membrane, creating a permanent irreversible damage [44], while maintaining the cell's architecture: the nucleus, the mitochondria and other cellular organelles are always present. A significant difference is observable between an untreated cell and a treated cell, on both parameters (ΔC and ΔG). The saponin-treated cells have less contrast than the untreated cells. In the case of cells treated with saponin, which will be considered as our positive control for the rest of the study, the cell membrane becomes permeable. Under the effect of the osmotic pressure linked to the difference in concentrations between the intra- and extracellular species, an equilibrium is created between the two compartments. The cytosolic composition is therefore greatly impacted, which results in a lower contrast between the extracellular and intracellular media compared to untreated cells. This results in a decrease (in absolute values) of the capacitive and conductive contrasts.

Thus, using our biosensor, we are able to highlight the presence of a living cell in its liquid culture medium, as well as permeabilized cells, presenting different dielectric responses. Table 1 summarizes the capacitive and conductive contrasts, at 5 GHz and 30 GHz respectively, of THP-1 cell line, with standard deviation values. Around fifty cells have been tested for each condition. These frequencies are particularly chosen to have the maximum value of the two parameters and are consequently considered in the next sections specifically. This table also shows the value of the threshold values for C and G contrast parameters defining the living and dead (i.e., permeabilized) characters of cells. These threshold values were defined in the middle of the measured dynamics of the living cell batches versus the saponin treated ones. This threshold will be used in the rest of the study for cell screening depending on the viability.

B. Dielectric properties of THP-1 cells treated with electrochemotherapy

As explained earlier, one of the applications of electroporation is to facilitate the transport of low or non-permeant molecules through the cell membrane and thus

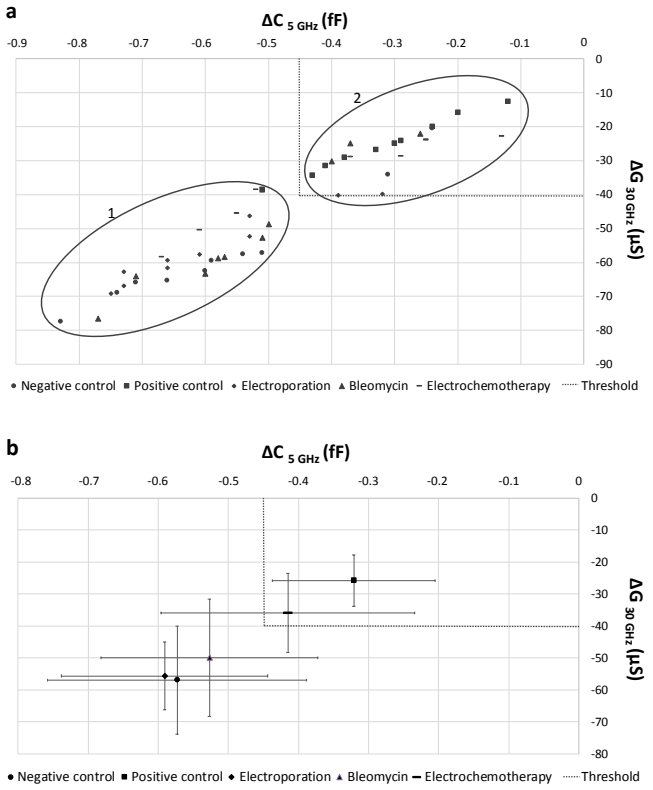

Fig. 8. Position of the different measurements of THP-1 cells undergoing different treatments, in the complex plane (ΔC5GHz, ΔG30 GHz) (a) without and (b) with the standard deviations of measurement.

potentiate the cytotoxic effect of anti-tumor drugs (electrochemotherapy). The aim of this study is to evaluate the ability of our microwave biosensor to detect the loss of cell viability induced by the entry of bleomycin molecules after electroporation. Thus, THP-1 cells are treated with either bleomycin alone, electroporation alone, or electrochemotherapy (bleomycin + EP). The different dielectric responses are compared to those of untreated cells (negative control) and saponin-treated cells (positive control). Fig. 5 and Fig. 6 show, respectively, capacitive contrast (ΔC) and conductive contrast (ΔG) spectra obtained for different conditions of treatment. A small but representative number of spectra is presented in these figures, in order to give a general idea of the spectral behavior of the cells as well as the measurement repeatability. By comparing the treated cell spectra to the negative control cell spectra (Fig. 4) in a qualitative manner, we observe a decrease in absolute values of ΔC (Fig. 5.a) and ΔG (Fig. 5.b) for some cells, especially those treated with ECT. It creates a distinct separation between two cell subgroups: living cells and cells affected by the ECT treatment.

In order to consolidate our observations, a quantitative study of the obtained results is made. Therefore, we proceed to a cell sorting and a classification based on the thresholds established earlier. Fig. 6.a and Fig. 6.b show the evolution of the mean values of the capacitive and conductive contrasts, respectively, at the selected frequencies (5 GHz and 30 GHz), as a function of the treatment condition. The percentages of

living and affected cells are also shown on the graphs. In comparison to the negative control cells, which feature a viability rate around 80%, we can clearly establish that when cells are treated with bleomycin alone or subjected to the electric field alone, the resulting viability is not significantly affected (~72%, ~80%), whereas treating cells with bleomycin coupled to the electric field causes an increase in the number of cells exceeding the threshold and exhibiting electrical responses characteristic of dead cells (~53%). The same behavior is observed on the conductive contrast ΔG, where ECT induces a clear decrease in viability down to ~36%.

In order to further validate our results and the efficacy of our biosensor, we compare and correlate the evolution of the viability rates obtained with microwave measurements ($\Delta C_{5\ GHz}$ and $\Delta G_{30\ GHz}$) to the standard biological exclusion test with trypan blue. Indeed, there is a concordance in the results obtained with the two techniques, as shown in Fig. 7. Statistical analysis reveals a very good correlation between the two methods of analysis ($R^2_{\ \Delta C/Exclusion\ test}$ = 0.97) / ($R^2_{\ \Delta G/Exclusion\ test}$ = 0.99), indicating the reliability of microwave dielectric spectroscopy for detecting the effect of electrochemotherapy on THP1 cells.

C. Single cell analysis

Biological studies have been for long performed on groups of cells assuming that all cells of a particular "type" are identical. However, studies on individual cells reveal that this assumption is incorrect. Individual cells within the same population can vary considerably [45]–[47]. This is called "individuality" of cells within the population [48]. These differences can have important consequences for the understanding of certain diseases, since certain singular cells play a fundamental role in the pathogenesis of the disease, its evolution over time and in the sensitivity of cells to drugs. New approaches to single-cell analysis are therefore crucial to discover fundamental biological principles and, as a result, improve the detection and treatment of diseases.

The measurements we obtained in our study are represented in a complex plane ($\Delta C_{5\ GHz}$, $\Delta G_{30\ GHz}$), as shown in Fig. 8.a. We identify a distribution in two clouds of measuring points, based on the threshold values established earlier. The first cloud (1) brings together living cells and the second one (2) contains affected (i.e. dead) cells. By calculating the mean values and the standard deviations of the measurements for each condition (Fig. 8.b), we note that the untreated cells, along with the cells treated with bleomycin or electroporation alone, have a mean value that lies outside the designated affected box, whereas the mean values of the cells treated with saponin or electrochemotherapy lie inside of this box. The mixture of living and affected cells in this population gives a mean value that does not reflect the true state of the two subpopulations of cells: this means that a global study of cell populations masks information when cell suspensions become heterogeneous, hence the interest of a study at the level of the single cell.

IV. Conclusions

This paper presents an original single cell biosensor based on microwave spectroscopy for the dielectric characterization of human cells subjected to electrochemotherapy. Our biosensor is designed for a label-free detection and an effective measurement of frequency-dependent cell-based parameters (C_{cell} (f) and G_{cell} (f)) of THP-1 cells subjected to different types of treatment. With our biosensor, we are able to reveal the potentiation of the bleomycin molecule with the application of electric pulses (electrochemotherapy). Aside from dielectric measurements, comparison with standard biological tests (based on the exclusion test with trypan blue) points out a strong correlation between the two methods (R^2>0.97). These findings indicate the robustness and the reliability of microwave dielectric spectroscopy for label-free biological and medical analysis, and that it may be very helpful to provide deeper insights on the effect of electrochemotherapy on cancer and healthy cells and to optimize electric pulses parameters to ensure efficient cancer cell eradication whatever the cell type and population heterogeneity.

References

[1] L. M. Mir, S. Orlowski, J. Belehradek, and C. Paoletti, "Electrochemotherapy potentiation of antitumour effect of bleomycin by local electric pulses," *Eur. J. Cancer Clin. Oncol.*, vol. 27, no. 1, pp. 68–72, Jan. 1991, doi: 10.1016/0277-5379(91)90064-K.

[2] G. Sersa, Gregor, M. Cemaiar, and D. Miklavcic, "Antitumor Effectiveness of Electrochemotherapy with cis-Diamminedichloroplatinum(II) in Mice!," *Cancer Res.*, vol. 55, pp. 3450–3455, Aug. 1995.

[3] A. Testori *et al.*, "Electrochemotherapy for cutaneous and subcutaneous tumor lesions: a novel therapeutic approach: ECT for skin tumors," *Dermatol. Ther.*, vol. 23, no. 6, pp. 651–661, Nov. 2010, doi: 10.1111/j.1529-8019.2010.01370.x.

[4] L. M. Mir, "Therapeutic perspectives of in vivo cell electropermeabilization," *Bioelectrochemistry Amst. Neth.*, vol. 53, no. 1, pp. 1–10, Jan. 2001.

[5] O. Tounekti, G. Pron, J. Belehradek, and L. M. Mir, "Bleomycin, an apoptosis-mimetic drug that induces two types of cell death depending on the number of molecules internalized," *Cancer Res.*, vol. 53, no. 22, pp. 5462–5469, Nov. 1993.

[6] J. Gehl, T. Skovsgaard, and L. M. Mir, "Enhancement of cytotoxicity by electropermeabilization: An improved method for screening drugs," *Anticancer. Drugs*, vol. 9, no. 4, pp. 319–325, Jun. 1998.

[7] E. P. Spugnini, G. Citro, P. Mellone, I. Dotsinsky, N. Mudrov, and A. Baldi, "Electrochemotherapy for localized lymphoma: a preliminary study in companion animals," *J. Exp. Clin. Cancer Res. CR*, vol. 26, no. 3, pp. 343–346, Sep. 2007.

[8] J. Gehl, "Electroporation: theory and methods, perspectives for drug delivery, gene therapy and research," *Acta Physiol. Scand.*, vol. 177, no. 4, pp. 437–447, Apr. 2003, doi: 10.1046/j.1365-201X.2003.01093.x.

[9] G. Sersa and D. Miklavcic, "Electrochemotherapy of Tumours," *J. Vis. Exp.*, no. 22, p. 1038, Dec. 2008, doi: 10.3791/1038.

[10] S. Orlowski, J. Belehradek, C. Paoletti, and L. M. Mir, "Transient electropermeabilization of cells in culture: Increase of the cytotoxicity of anticancer drugs," *Biochem. Pharmacol.*, vol. 37, no. 24, pp. 4727–4733, Dec. 1988, doi: 10.1016/0006-2952(88)90344-9.

[11] L. M. Mir *et al.*, "[Electrochemotherapy, a new antitumor treatment: first clinical trial]," *C. R. Acad. Sci. III*, vol. 313, no. 13, pp. 613–618, 1991.

[12] A. Gothelf, L. M. Mir, and J. Gehl, "Electrochemotherapy: results of cancer treatment using enhanced delivery of bleomycin by electroporation," *Cancer Treat. Rev.*, vol. 29, no. 5, pp. 371–387, Oct. 2003, doi: 10.1016/S0305-7372(03)00073-2.

[13] F. Maglietti *et al.*, "Electroporation as the Immunotherapy Strategy for Cancer in Veterinary Medicine: State of the Art in Latin America," *Vaccines*, vol. 8, no. 3, p. 537, Sep. 2020, doi: 10.3390/vaccines8030537.

[14] G. Sersa *et al.*, "Outcomes of older adults aged 90 and over with

cutaneous malignancies after electrochemotherapy with bleomycin: A matched cohort analysis from the InspECT registry," *Eur. J. Surg. Oncol.*, vol. 47, no. 4, pp. 902–912, Apr. 2021, doi: 10.1016/j.ejso.2020.10.037.
[15] D. Scala *et al.*, "Electrochemotherapy for rectal cancer after neoadjuvant radiotherapy: A case report," *Eur. J. Surg. Oncol. EJSO*, vol. 41, no. 1, pp. S13–S14, Jan. 2015, doi: 10.1016/j.ejso.2014.10.037.
[16] I. Edhemovic *et al.*, "Intraoperative electrochemotherapy of colorectal liver metastases," *J. Surg. Oncol.*, vol. 110, no. 3, pp. 320–327, Sep. 2014, doi: 10.1002/jso.23625.
[17] D. Ágoston *et al.*, "Evaluation of Calcium Electroporation for the Treatment of Cutaneous Metastases: A Double Blinded Randomised Controlled Phase II Trial," *Cancers*, vol. 12, no. 1, p. 179, Jan. 2020, doi: 10.3390/cancers12010179.
[18] M. Khine, A. Lau, C. Ionescu-Zanetti, J. Seo, and L. P. Lee, "A single cell electroporation chip," *Lab. Chip*, vol. 5, no. 1, p. 38, 2005, doi: 10.1039/b408352k.
[19] S. Kar *et al.*, "Single-cell electroporation: current trends, applications and future prospects," *J. Micromechanics Microengineering*, vol. 28, no. 12, p. 123002, Dec. 2018, doi: 10.1088/1361-6439/aae5ae.
[20] Y. Ye *et al.*, "Single-Cell Electroporation with Real-Time Impedance Assessment Using a Constriction Microchannel," *Micromachines*, vol. 11, no. 9, p. 856, Sep. 2020, doi: 10.3390/mi11090856.
[21] L. Chang *et al.*, "Micro-/nanoscale electroporation," *Lab. Chip*, vol. 16, no. 21, pp. 4047–4062, 2016, doi: 10.1039/C6LC00840B.
[22] T. Geng and C. Lu, "Microfluidic electroporation for cellular analysis and delivery," *Lab Chip*, vol. 13, no. 19, pp. 3803–3821, Jul. 2013, doi: 10.1039/C3LC50566A.
[23] A. Hai and M. E. Spira, "On-chip electroporation, membrane repair dynamics and transient in-cell recordings by arrays of gold mushroom-shaped microelectrodes," *Lab. Chip*, vol. 12, no. 16, p. 2865, 2012, doi: 10.1039/c2lc40091j.
[24] J. Ghosh, X. Liu, and K. D. Gillis, "Electroporation followed by electrochemical measurement of quantal transmitter release from single cells using a patterned microelectrode," *Lab. Chip*, vol. 13, no. 11, p. 2083, 2013, doi: 10.1039/c3lc41324a.
[25] R. Connolly, J. Rey, M. Jaroszeski, A. Hoff, R. Gilbert, and J. Llewellyn, "Effectiveness of non-penetrating electroporation applicators to function as impedance spectroscopy electrodes," *IEEE Trans. Dielectr. Electr. Insul.*, vol. 16, no. 5, pp. 1348–1355, Oct. 2009, doi: 10.1109/TDEI.2009.5293948.
[26] C. I. Trainito, O. Français, and B. Le Pioufle, "Monitoring the permeabilization of a single cell in a microfluidic device, through the estimation of its dielectric properties based on combined dielectrophoresis and electrorotation in situ experiments: Microfluidics and Miniaturization," *ELECTROPHORESIS*, vol. 36, no. 9–10, pp. 1115–1122, May 2015, doi: 10.1002/elps.201400482.
[27] S. C. Bürgel, C. Escobedo, N. Haandbæk, and A. Hierlemann, "On-chip electroporation and impedance spectroscopy of single-cells," *Sens. Actuators B Chem.*, vol. 210, pp. 82–90, Apr. 2015, doi: 10.1016/j.snb.2014.12.016.
[28] M. Khine, C. Ionescu-Zanetti, A. Blatz, L.-P. Wang, and L. P. Lee, "Single-cell electroporation arrays with real-time monitoring and feedback control," *Lab. Chip*, vol. 7, no. 4, p. 457, 2007, doi: 10.1039/b614356c.
[29] K. Grenier *et al.*, "Recent Advances in Microwave-Based Dielectric Spectroscopy at the Cellular Level for Cancer Investigations," *IEEE Trans. Microw. Theory Tech.*, vol. 61, no. 5, pp. 2023–2030, May 2013, doi: 10.1109/TMTT.2013.2255885.
[30] F. Artis *et al.*, "Microwaving Biological Cells: Intracellular Analysis with Microwave Dielectric Spectroscopy," *IEEE Microw. Mag.*, vol. 16, no. 4, pp. 87–96, May 2015, doi: 10.1109/MMM.2015.2393997.
[31] E. Levy, G. Barshtein, L. Livshits, P. B. Ishai, and Y. Feldman, "Dielectric Response of Cytoplasmic Water and Its Connection to the Vitality of Human Red Blood Cells: I. Glucose Concentration Influence," *J. Phys. Chem. B*, vol. 120, no. 39, pp. 10214–10220, Oct. 2016, doi: 10.1021/acs.jpcb.6b06996.
[32] Poiroux G. et al., "Label-free Detection of Mitochondrial Activity with Microwave Dielectric Spectroscopy," *Int. J. Biotechnol. Bioeng.*, vol. 6, no. 5, Jul. 2020.
[33] K. Grenier *et al.*, "Integrated Broadband Microwave and Microfluidic Sensor Dedicated to Bioengineering," *IEEE Trans. Microw. Theory Tech.*, vol. 57, no. 12, pp. 3246–3253, Dec. 2009, doi: 10.1109/TMTT.2009.2034226.
[34] Y. Yang *et al.*, "Distinguishing the viability of a single yeast cell with an ultra-sensitive radio frequency sensor," *Lab. Chip*, vol. 10, no. 5, p. 553, 2010, doi: 10.1039/b921502f.
[35] T. Chen, F. Artis, D. Dubuc, J. J. Fournié, M. Poupot, and K. Grenier, "Microwave biosensor dedicated to the dielectric spectroscopy of a single alive biological cell in its culture medium," in *2013 IEEE MTT-S International Microwave Symposium Digest (MTT)*, Jun. 2013, pp. 1–4. doi: 10.1109/MWSYM.2013.6697740.
[36] S. Afshar, E. Salimi, K. Braasch, M. Butler, D. J. Thomson, and G. E. Bridges, "Multi-Frequency DEP Cytometer Employing a Microwave Sensor for Dielectric Analysis of Single Cells," *IEEE Trans. Microw. Theory Tech.*, pp. 1–9, 2016, doi: 10.1109/TMTT.2016.2518178.
[37] N. Meyne, G. Fuge, A.-P. Zeng, and A. F. Jacob, "Resonant Microwave Sensors for Picoliter Liquid Characterization and Nondestructive Detection of Single Biological Cells," *IEEE J. Electromagn. RF Microw. Med. Biol.*, vol. 1, no. 2, pp. 98–104, Dec. 2017, doi: 10.1109/JERM.2017.2787479.
[38] X. Ma, X. Du, H. Li, X. Cheng, and J. C. M. Hwang, "Ultra-Wideband Impedance Spectroscopy of a Live Biological Cell," *IEEE Trans. Microw. Theory Tech.*, vol. 66, no. 8, pp. 3690–3696, Aug. 2018, doi: 10.1109/TMTT.2018.2851251.
[39] G. Chen *et al.*, "Conductivity in Jurkat cell suspension after ultrashort electric pulsing," Jan. 2004.
[40] A. L. Garner *et al.*, "Ultrashort electric pulse induced changes in cellular dielectric properties," *Biochem. Biophys. Res. Commun.*, vol. 362, no. 1, pp. 139–144, Oct. 2007, doi: 10.1016/j.bbrc.2007.07.159.
[41] A. Tamra, D. Dubuc, M.-P. Rols, and K. Grenier, "Microwave Monitoring of Single Cell Monocytes Subjected to Electroporation," *IEEE Trans. Microw. Theory Tech.*, vol. 65, no. 9, pp. 3512–3518, Sep. 2017, doi: 10.1109/TMTT.2017.2653776.
[42] H. Li, X. Ma, X. Du, L. Li, X. Cheng, and J. C. M. Hwang, "Correlation Between Optical Fluorescence and Microwave Transmission During Single-Cell Electroporation," *IEEE Trans. Biomed. Eng.*, vol. 66, no. 8, pp. 2223–2230, Aug. 2019, doi: 10.1109/TBME.2018.2885781.
[43] M. Marty *et al.*, "Electrochemotherapy – An easy, highly effective and safe treatment of cutaneous and subcutaneous metastases: Results of ESOPE (European Standard Operating Procedures of Electrochemotherapy) study," *Eur. J. Cancer Suppl.*, vol. 4, no. 11, pp. 3–13, Nov. 2006, doi: 10.1016/j.ejcsup.2006.08.002.
[44] I. Podolak, A. Galanty, and D. Sobolewska, "Saponins as cytotoxic agents: a review," *Phytochem. Rev.*, vol. 9, no. 3, pp. 425–474, Sep. 2010, doi: 10.1007/s11101-010-9183-z.
[45] D. D. Carlo and L. P. Lee, "Dynamic Single-Cell Analysis for Quantitative Biology," *Anal. Chem.*, vol. 78, no. 23, pp. 7918–7925, Dec. 2006, doi: 10.1021/ac069490p.
[46] D. G. Spiller, C. D. Wood, D. A. Rand, and M. R. H. White, "Measurement of single-cell dynamics," *Nature*, vol. 465, no. 7299, pp. 736–745, Jun. 2010, doi: 10.1038/nature09232.
[47] D. Bakstad, A. Adamson, D. G. Spiller, and M. R. White, "Quantitative measurement of single cell dynamics," *Curr. Opin. Biotechnol.*, vol. 23, no. 1, pp. 103–109, Feb. 2012, doi: 10.1016/j.copbio.2011.11.007.
[48] J. Zhao, "Cell individuality: A basic multicellular phenomenon and its role in the pathogenesis of disease," *Med. Hypotheses*, vol. 44, no. 5, pp. 400–402, May 1995, doi: 10.1016/0306-9877(95)90267-8.